



Iranian Research Organization  
for Science and Technology  
(IROST)

Advances  
Environmental  
Technology



Journal home page: <https://aet.irost.ir/>

# Characterisation and source apportionment of atmospheric particulate matter in an industrial cluster of Western India

Seema Nihalani, Namrata Jariwala\*, Anjali Khembete

Research Scholar Civil Engineering Department S V National Institute of Technology, Icchanath, Surat Gujarat, India

## ARTICLE INFO

### Document Type:

Research Paper

### Article history:

Received 23 October 2022

Received in revised form

20 August 2023

Accepted 9 September 2023

### Keywords:

Particulate matter

Receptor model

CMB

PMF

Vapi

## ABSTRACT

Pollution from atmospheric particulates is a severe environmental problem of universal concern. Fine and ultra-fine particulates harbour the ability to enter the bloodstream and carry with them trace metals like copper, cadmium, iron, lead, and zinc that can cause toxic and carcinogenic effects. This necessitates an increased emphasis on the detailed chemical characterisation of atmospheric particulates. The current study identified six locations in the Vapi industrial area. In these six locations, coarse particulate matter (PM<sub>10</sub>) samples were collected simultaneously for 20 days to determine the Elemental Carbon (EC), Organic Carbon (OC), Water-soluble ions (WSIs), and major and trace elements. The concentration of PM<sub>10</sub> was observed to be in the range of 115.88 to 226.5  $\mu\text{g}/\text{m}^3$ , exceeding the NAAQS standard value of 100  $\mu\text{g}/\text{m}^3$ . The chemical analysis results suggested contributions from total carbon, water-soluble ions, and elements varied between 45 to 48%, 20 to 23%, and 29 to 33% of PM<sub>10</sub> mass, respectively. Chemical mass balance (CMB) and Positive matrix factorisation (PMF) models were employed separately for carrying out source apportionment studies. CMB demonstrated influence from various sources: 35% from fossil fuel combustion that included industries, 22.90% from crustal or soil dust, 19.12% from biomass burning, 16.18% from vehicular emissions, and 6.79 % from secondary particulates. The PMF receptor model showed the influence from various sources as 25.75 % from fossil fuel combustion, 22.13 % from crustal or soil dust, 16.95% from vehicular emissions, 14.53% from biomass burning, 11.49% from industrial emissions, and 9.16% from secondary aerosols. Thus, this study shall help in formulating pollution abatement strategies.

## 1. Introduction

Rapid industrialization, urbanization, fossil fuel combustion, and economic growth have

substantially increased airborne particulates and other gaseous pollutants, especially in countries like India [1]. Various stern actions have already been initiated to curb the menace of air pollution;

\*Corresponding author:

E-mail: [ndj@ced.svnit.ac.in](mailto:ndj@ced.svnit.ac.in)

DOI: 10.22104/AET.2023.5917.1627

COPYRIGHTS: ©2023 Advances in Environmental Technology (AET). This article is an open access article distributed under the terms and conditions of the Creative Commons Attribution 4.0 International (CC BY 4.0) (<https://creativecommons.org/licenses/by/4.0/>)

however, many urban towns and cities are still facing this problem [2-4]. The respirable fraction of suspended particulate matter, which is termed PM10 or PM2.5, can be absorbed into human lungs while breathing, leading to several respiratory and cardiovascular health problems [5]. The chemical composition of airborne particulate matter, particularly heavy metal tracer markers, is of significant concern due to its acute and chronic adverse health effects [6]. The chief artificial sources of particulate pollution shall comprise traffic emissions, emissions from industries, combustion of fuels, construction activities, suspended and re-suspension dust, etc. [7]. Therefore, particulate matter concentration and its elemental speciation in ambient air reveal the features of activities involved, providing information regarding human exposure to such heavy metal pollution. Exhaustive monitoring programs involving different elements and heavy metals in urban particulates have been taken up worldwide in the past few years. These monitoring programs concentrated on the chemical characteristics and composition of particulates in addition to analysing continuing temporal trends. Further, classifying of particulate matter sources is essential for developing air pollution control and abatement strategies. Researchers have applied different tools for the source identification and computation of atmospheric particulate matter [08]. The estimation of different particulate sources, along with their contributions, is the chief concern in air quality research. Receptor modeling is one of the focal methods applied for source apportionment of particulate pollutants at any sampling site [3,9]. Different models, including CMB, Principal Component Analysis (PCA), UNMIX, and PMF, have been used by several researchers for identifying the source contribution of urban particulates [10,11]. The Gujarat Industrial Development Corporation (GIDC) developed the Vapi industrial estate in Valsad, with a total area of 1140 hectares and in close vicinity to NH8 and the Delhi-Mumbai rail corridor. Looking at its location and development over the years, Vapi plays an important role in the industrial activities and economic growth of Gujarat as well as India. However, over the years, it has earned the reputation of being one of the most polluted

industrial stretches in the country. The Central Pollution Control Board (CPCB) has formulated the concept of the Comprehensive Environmental Pollution Index (CEPI) for analysis of the environmental status of the various industrial clusters across India [12]. With an overall CEPI score of 89.09 for the year 2019-2020, Vapi has been classified as a very critically polluted cluster [12]. Within the last two years, the concentration of PM10 and PM2.5 in Vapi was beyond the permissible limit for the majority of the year [12]. Various action plans and mitigation measures, including air quality monitoring and measuring the impact on the health of surrounding populations, have turned out to be futile [13]. This has created a need for a detailed study of the critically polluted industrial cluster of Vapi. Therefore, in order to transform Vapi from a non-attainment city to an attainment city, a source apportionment study is the need of the hour. As per CPCB sources, Vapi houses around 1400 industrial units, of which 800 units are operational [13]. Around 70 percent of these industries produce pharmaceuticals, pigments, dyes, pigments, and pesticides, whereas the remaining 30 percent comprise other small-scale industries like engineering, plastic, paper mills, and packaging [13]. These industries use different kinds of fuels, like coke, lignite, firewood, furnace oil, light diesel oil, etc. Due to the presence of such heterogeneous kinds of industries and the utility of such different fuels, the resulting source profiles shall be complex in nature and difficult to develop. Furthermore, the studies on source apportionment using the CMB model are rather limited in India [14]. This paper attempted to assess the various sources of coarse particulates in Vapi using CMB and PMF receptor models. The current study presents the chemical characterisation of atmospheric PM for the Vapi industrial area from Dec 2019 to Jan 2020, consisting of EC, OC, water-soluble ions that include cations and anions, and major and trace elements, along with source apportionment of PM10 mass. The current study focused on the winter season because it is believed to be the worst time of year for the dispersion of air pollution [4]. Additionally, because the study encompassed an industrial area, where the industries worked the full day, there would be very little influence on the air pollutants concerning

meteorological parameters. Consequently, source apportionment studies using CMB and PMF shall serve the purpose of source identification and quantification with the existing information and data sets available.

## 2. Site description

The study area for Vapi was from latitude - 20°23'47.63"N and longitude - 72°53'22.40"E until latitude -20°20'16.79"N and longitude-72°57'20.55"E, with a mean sea elevation of about 30 metres. Vapi has a mean annual temperature of 27 °C, with an annual mean relative humidity of 70% and annual average precipitation of 2000 mm. The annual average wind velocity is 3.6 m/s, and the predominant wind direction is West-South-west for the maximum time of the year (Source: <https://www.worldweatheronline.com/>). The details of the sampling locations selected in the study area are shown in Table 1 and Figure 1. The stations were selected to cover all the major areas of Vapi, which is the extent of the study area. The stations were also based to consider satisfactory safety measures and lower intervention of the local public with the sampling devices. Respirable and fine dust samplers were used to monitor the particulate concentration at all six sampling locations. Further chemical analysis of PM10 filter papers was done to determine the elemental concentration of NO<sub>3</sub><sup>-</sup>, SO<sub>4</sub><sup>-2</sup>, NH<sub>4</sub><sup>+</sup>, K-S<sup>+</sup>, Na, EC, OC, Al, Br, Ca<sup>+2</sup>, Cl, Cr, Cu, Fe, K<sup>+</sup>, Mn, Ni, Pb, S, Si, Ti, V, and Zn.

## 3. Methodology-Sampling and Chemical Analysis

The sampling of PM<sub>10</sub> was done by means of a respirable dust sampler, APM – 415BL. The sampling of PM<sub>2.5</sub> was done using APM-550 at the six locations shown in Figure 1 from Dec. 2019 to Jan. 2020. The monitoring was carried out simultaneously at all six locations from Dec. 19, 2019, to Jan. 7, 2020, for a period of 20 days. The PM<sub>10</sub> samples were collected on Quartz filter QM-A papers having a size of 20.3 x 25.4 cm<sup>2</sup> and a rate of flow of 1.13 m<sup>3</sup>/min with ± 2% accuracy for 24 hours of sampling. The PM<sub>2.5</sub> samples were collected on Teflon (PTFE – Polytetrafluoroethylene) papers having a 47 mm size and a rate of flow of 16.6 lpm with ± 2% accuracy for 24 hours of sampling. Thus, 120 samples for PM<sub>10</sub> and PM<sub>2.5</sub> were gathered for all six locations. The filter papers utilised in particulate matter monitoring were conditioned at 25°C and 50% relative humidity for two days in a desiccator. The conditioning of the filter papers was done before and after sampling. The gravimetric weight of filter papers was taken using a five-digit weighing balance. The systematic methods involved in this study were:

- Gravimetric analysis for particulate matter concentration,
- Ion Chromatograph for WSI analysis,
- Inductively coupled plasma-atomic emission spectrometer (ICP-AES) for element analysis, and
- EC-OC carbon analyser for elemental and organic carbon analysis.

**Table 1.** Details of sampling locations.

Station	Details	Name	Land-use category	Latitude	Longitude
1	Location-1	AQ1	Commercial	N 20° 21' 54.3"	E 072° 54' 25.7"
2	Location-2	AQ2	Green cover	N 20 °20' 46.8"	E 072° 55' 30.7"
3	Location-3	AQ3	Industrial	N 20° 21' 50.5"	E 072° 56' 0.26"
4	Location-4	AQ4	Industrial	N 20°22' 08.6"	E 072° 57' 01.1"
5	Location-5	AQ5	Industrial	N 20° 20' 54.6"	E 072° 56' 15.9"
6	Location-6	AQ6	Industrial	N 20° 22' 24.8"	E 072° 55' 41.0"

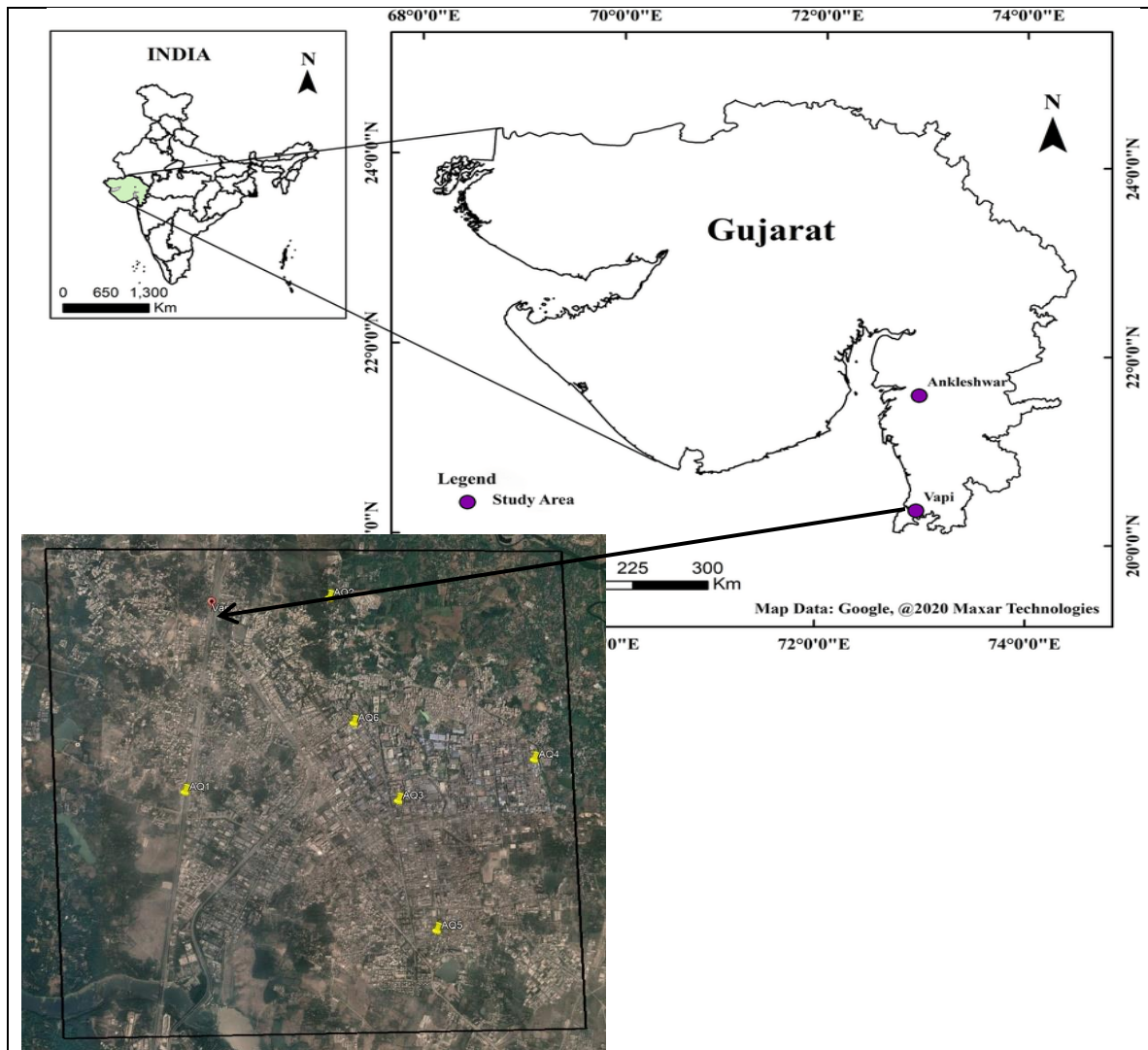


Fig. 1. Ambient air quality locations.

After determining the particulate matter concentration, the  $PM_{10}$  filter papers were divided into three parts. The first part was used for the analysis of the elements, the second part was used for ion analysis, and the remaining third part was utilised for EC-OC investigation.

- a. A hot plate was used to carry out digestion for further extraction of elements from the filter papers [15]. After the digestion of one-third filter paper, sample filtration was carried out using Whatman filter paper, and the sample was further stored in a refrigerator for analysis. The separated and refrigerated sample was analysed using an ICP-AES (Jobin Yvon, Model ULTIMA 2000), and the analysis of 15 metallic elements, namely Al, Br, S, Si, Ti, Cl, Cr, Cu, Fe, Mn, Na, Ni, Pb, V, and Zn, was carried out.
- b. For ion analysis, the second part of the filter paper was used for analysis as per the standard procedure recommended by CPCB [15]. This one-third part of the filter was extracted using ultra-pure or deionized water with a resistivity of 18 MU. The extracted water sample was filtered using a syringe filter and stored for further analysis. Finally, the filtered and extracted samples were analysed with an ion chromatograph (IC Basic 792: Metrohm) to determine the water-soluble ions under optimum conditions. Four cations- ammonium ( $NH_4^+$ ), potassium ( $K^+$ ), potassium ( $K-S^+$ ) salt, and calcium ( $Ca^{+2}$ ) and two anions- nitrate ( $NO_3^-$ ) and sulfate ( $SO_4^{-2}$ ) were included in the ion analysis.
- c. The third and remaining part of the filter paper was analysed using an EC – OC carbon analyser

(model DRI2001, Protocol Improve A) using USEPA protocol [8]. The EC/OC carbon analyser works on the principle of controlled oxidation of EC and OC and liberating the carbon complexes at different temperatures. For quality control and assurance purposes, the standard reference materials and filter blanks were subject to analytical protocols.

#### 4. Receptor models

##### 4.1. CMB receptor model

The CMB model uses the least-squares regression approach to ascertain the probable sources of particulate matter [11]. This method was initially proposed by Winchester and Nifong in 1971 and later used by Miller in 1972. The basis of the CMB method is mass conservation, which can be used for the source apportionment of particulate matter in the atmosphere [10,16]. The fundamental principle behind this method assumes that while traveling from the source to the receptors, the signature markers do not transform chemically [17]. This method assumes that the concentration at any receptor is a direct summation of the source profile and can be determined when suitable uncertainty estimations exist [18]. The CMB model uses several linear regression algorithms to provide different source contributions from source and receptor profiles as well as relevant uncertainties. [19]. However, while selecting the source profiles, proper care must be taken to elude linearity and the likelihood of identical geographical areas; otherwise, the relevance of the model will be reduced substantially. In order to reduce the linearity of source profiles, grouping or combining similar sources is suggested. CMB is one of the fundamental receptor modeling techniques used for source apportionment studies, and it gives appropriate results even when limited datasets are available [20]. The input of comprehensive source profiles facilitates the requirement of fewer data monitoring sets; however, it shall escalate the associated level of uncertainties. The CMB model is represented by Equation 1 shown below:

$$C_{ik} = \sum_{n=1}^N F_{in} S_{kn} \quad (1)$$

where  $C_{ik}$  = species concentration of  $i$ th species from  $k$ th source,  $S_{kn}$  = influence from the  $k^{\text{th}}$  source,

and  $F_{in}$  = identified source profile. The CMB model uses the following assumptions: (i) during ambient and source sampling, source emission compositions are assumed to be constant; (ii) there is no reaction between the chemical species; (iii) all sources having a probable contribution to the receptor has been recognized and characterisation of emissions performed; (iv) the number of sources shall be less than the number of species; (v) the source profiles shall not be linearly dependent on each other; and (vi) there shall be normal distribution and no correlation between the random uncertainties [21].

##### 4.2. PMF receptor model

In the current study, Positive matrix factorization (PMF version 5.0, by USEPA) was applied to compute the different source contributions to the  $PM_{10}$  mass for the Vapi industrial area in Gujarat. PMF is a powerful multivariate receptor model that can carry out the apportionment of sources efficiently without prior knowledge about the sources [22,23]. It works on the principle of reducing a speciated input data matrix into two resulting sub-matrices representing factor profiles and factor contributions [8,24]. The PMF receptor model usually involves two different input files; the first input file consists of different species concentrations as measured, and the second input file consists of estimated uncertainties for species concentration [25,26]. The input data matrix  $X$  is generally viewed as having order  $i \times j$ , where  $i$  denotes the total number of samples and  $j$  denotes the total number of measured species. As stated above, the objective of using PMF analysis is to decompose input matrix  $X$  into two resulting matrices [15]. The resulting matrices are denoted by  $g$  and  $f$  ( $X = g \times f + e$ ), where  $g$  has the dimensions  $i \times p$ , and matrix  $f$  has dimensions  $p \times j$ , with  $p$  representing the number of extracted factors [9]. This can be represented by Equation 2:

$$X_{ij} = \sum_{k=1}^p g_{ik} f_{kj} + e_{ij} \quad (2)$$

where  $e_{ij}$  represents the residual value in every sample [20].

PMF allocates weight to every data point individually [27]. This aspect helps the user modify the impact of every data point for each

measurement based on its confidence interval. For instance, the data set having values lower than the detection limit shall be adjusted as per the associated uncertainty and then used in the model. As a result, the influence of these data points on the solution shall be fairly less compared to the measurements having values greater than the detection limit [28]. While applying PMF analysis, the objective function  $Q$  undergoes minimisation, depending upon the calculated uncertainties ( $u$ ), as depicted in Equation 3:

$$Q = \sum_{i=1}^n \sum_{j=1}^m \left[ \frac{X_{ij} - \sum_{k=1}^p g_{ik} f_{kj}}{u_{ij}} \right] \quad (3)$$

where  $X_{ij}$  = determined concentration ( $\mu\text{g}/\text{m}^3$ ),  $u_{ij}$  = associated uncertainty ( $\mu\text{g}/\text{m}^3$ ),  $p$  = number of factors extracted,  $j$  = total number of species, and  $i$  = total number of samples. The detailed description and working of PMF can be referred to in the EPA PMF Reference User Guide available with the software. For the present research work, data for the chemical characterisation of 23 species and 120  $\text{PM}_{10}$  samples were fed as input to the PMF multivariate model. The signal-to-noise ratio (S/N) and method detection limit (MDL) were computed as mentioned in the EPA reference guide, and the values are shown in Table 2. The EPA guide suggests that elements having values of S/N more than 2 are termed robust in the data class [29]. Further, species having an S/N ratio in between the range of 0.2 to 2 are termed to be shaky in the data class [30,31]. These weak species don't result in an adequate disparity in the concentrations; hence, the results are observed to have noise. The species having S/N ratios less than 0.2 are termed as poor values and are therefore not included in the analysis [32,33]. For the present study, all the elements had a value of S/N higher than 1.48, except Ni, with a value of 0.05. The range of scaled residuals was observed between +3 to -3 for all the species, and the  $Q_{\text{robust}}$  value was consistent with  $Q_{\text{true}}$ , indicating that the optimum  $Q$  base run shall be considered a reliable solution. To identify the errors in the optimum solution given by the PMF model, the Displacement (DISP), Bootstrap (BS), and Bootstrap displacement (BS-DISP) methods available in the software were used.

**Table 2.**  $R^2$ , S/N ratio, & Method Detection limit- MDL for  $Q$  robust run.

Species	S/N	$R^2$	MDL
EC	9.93	0.31	0.35
Pb	9.9	0.99	0.01
Ti	9.82	0.97	0.03
Si	9.59	0.64	0.12
OC	9.31	0.15	0.94
Br	9.27	0.04	0.01
Al	9.13	0.25	0.16
Cr	8.99	0.97	0.01
$\text{SO}_4^{-2}$	8.84	0.59	0.21
Fe	8.8	0.7	0.06
S	7.8	0.09	0.12
$\text{NO}_3^-$	6.84	0.04	0.28
$\text{NH}_4^+$	6.59	0.05	0.2
Cl	5.54	0.02	0.25
$\text{Ca}^{+2}$	5.09	0.08	0.29
$\text{K-S}^+$	4.8	0.03	0.46
V	4.77	0	0.01
Zn	4.74	0.07	0.07
Mn	3.71	0.07	0.01
$\text{K}^+$	2.25	0.02	0.46
Na	1.68	0.05	0.42
Cu	1.48	0.03	0.01
Ni	0.05	0	0.05

## 5. Results and discussion

### 5.1. Concentration of $\text{PM}_{10}$ and $\text{PM}_{2.5}$

The  $\text{PM}_{10}$  mass was collected on 20 quartz filter papers from Dec. 2019 – Jan. 2020 for each of the six locations, and further chemical analysis was carried out. The total  $\text{PM}_{10}$  concentration at the six locations varied between 115.87 to 226.5  $\mu\text{g}/\text{m}^3$ . The highest concentration of  $\text{PM}_{10}$  was observed at location 4, with the mean and standard deviation as  $226.50 \pm 38.70 \mu\text{g}/\text{m}^3$ , whereas the minimum concentration was observed at location 3 as  $115.88 \pm 21.85 \mu\text{g}/\text{m}^3$ . Further the mean  $\text{PM}_{10}$  concentration at other locations was  $207.10 \pm 34.62 \mu\text{g}/\text{m}^3$  for location 1,  $164.29 \pm 26.25 \mu\text{g}/\text{m}^3$  for location 2,  $188.85 \pm 31.07 \mu\text{g}/\text{m}^3$  for location 5, and  $144.87 \pm 23.41 \mu\text{g}/\text{m}^3$  for location 6. The concentration of  $\text{PM}_{2.5}$  for Vapi at six locations varied between 69.37 to 120.51  $\mu\text{g}/\text{m}^3$ , with an average value of about 94.69  $\mu\text{g}/\text{m}^3$ . The highest concentration of  $\text{PM}_{2.5}$  was observed at location 4, with mean and standard deviation as  $120.51 \pm 31.85$

$\mu\text{g}/\text{m}^3$ , whereas the minimum concentration was observed at location 3 as  $69.37 \pm 21.98 \mu\text{g}/\text{m}^3$ . Further, the mean  $\text{PM}_{2.5}$  concentration at other locations was observed as  $116.44 \pm 31.01 \mu\text{g}/\text{m}^3$  for location 1,  $92.21 \pm 25.12 \mu\text{g}/\text{m}^3$  for location 2,  $98.31 \pm 25.09 \mu\text{g}/\text{m}^3$  for location 5, and  $71.31 \pm 17.02 \mu\text{g}/\text{m}^3$  for location 6. Hence, the ratio of  $\text{PM}_{2.5}$  to  $\text{PM}_{10}$  in the study area was observed to be between 0.38 to 0.73, with an average of 0.54, indicating the influence of combustion-related activities in the study area. The  $\text{PM}_{10}$  and  $\text{PM}_{2.5}$  concentrations in the study area are shown in Figure 2.

### 5.2. Chemical characterisation of $\text{PM}_{10}$ and $\text{PM}_{2.5}$

The analysis of the chemical characterisation of  $\text{PM}_{10}$  revealed carbons, water-soluble ions, major elements, and trace elements to be the four basic components, as shown in Figure 2. Of the four identified components, the highest concentration was carbon fractions, followed by elements and water-soluble ions. The percentage of total carbon, which included EC and OC, varied between 45% to 48% of the  $\text{PM}_{10}$  mass at different locations, which could be attributed to combustion from vehicles,

DG sets, refuse burning, biomass burning, and emissions from industries in the upwind. The fraction of water-soluble ions comprising  $\text{SO}_4^{2-}$ ,  $\text{NO}_3^-$ ,  $\text{Ca}^{+2}$ ,  $\text{NH}_4^+$ ,  $\text{K-S}^+$ , and  $\text{K}^+$  in the ambient  $\text{PM}_{10}$  samples varied between 20% to 23% of  $\text{PM}_{10}$  mass [6,8,25,26]. The concentration of major elements varied between 28% to 32% of  $\text{PM}_{10}$  mass, and the concentration of trace elements varied between 1% to 2% of  $\text{PM}_{10}$  mass.

### 5.3. Carbons and water-soluble ions

The corresponding fractions of total carbon included EC and OC. The share of OC exceeded the share of elemental carbon (EC) for all the sampling locations, as shown in Figure. 3. The fraction of OC ranged between 54% to 61% of the total carbon, while the share of EC was observed to be between 39% to 46% of the total carbon at different monitoring locations. Station AQ5 (61%) exhibited the highest fraction of OC and the lowest fraction of EC (39%). Station AQ3 indicated the highest fraction of EC (46%) and the lowest share of OC (54%).

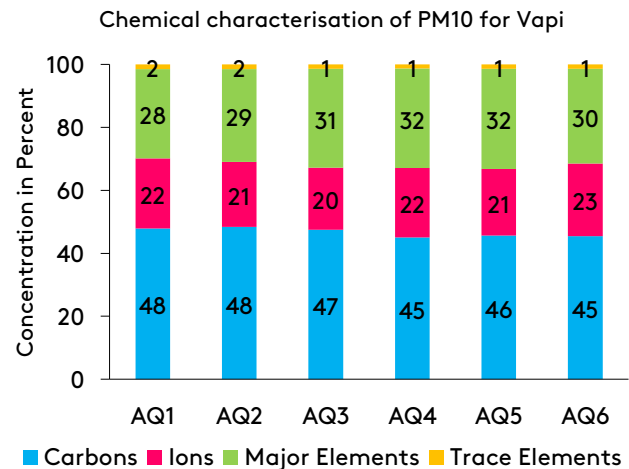
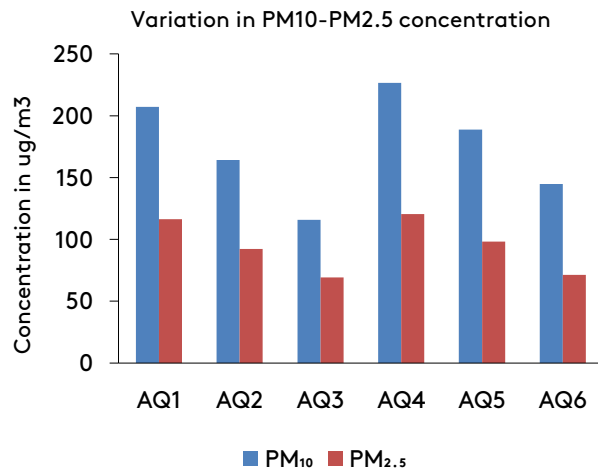


Fig. 2. Variation of  $\text{PM}_{10}$  -  $\text{PM}_{2.5}$  and chemical characterisation of  $\text{PM}_{10}$  for Vapi.

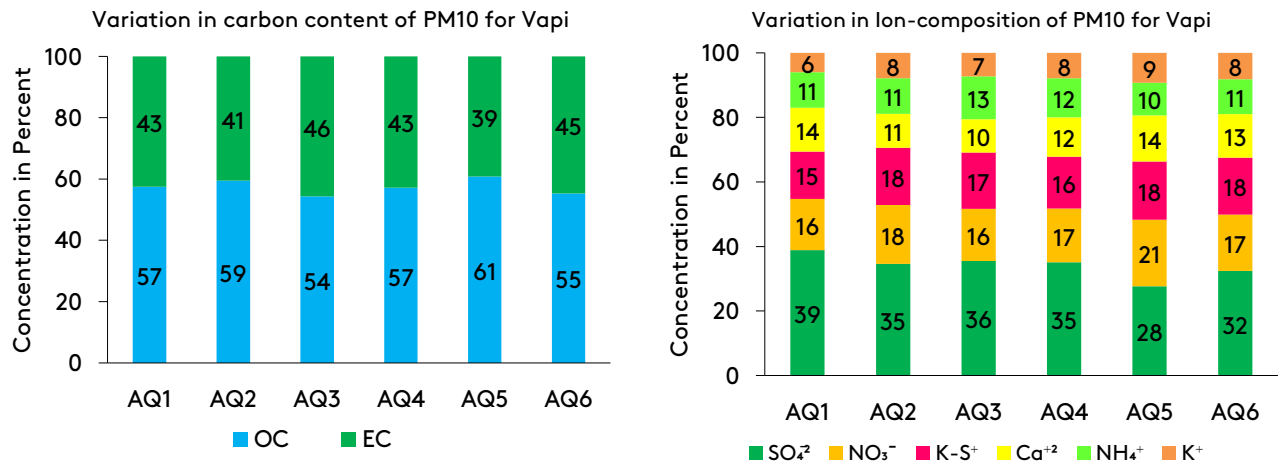


Fig. 3. Variation in carbon content and ion-composition of PM<sub>10</sub> for Vapi.

The native sources of elemental carbon can be industries, vehicles, refuse, or biomass burning, which release elemental carbon in substantial percentages along with organic carbon. The ambient concentration of OC and EC are considerably influence by emissions from vehicles and agricultural waste burning [30]. It is inferred that the value of OC/EC in the range of 1.4 to 4 implies gasoline vehicular emissions, and the value of an OC/EC ratio between 0.3 to 1 implies diesel vehicle emissions. For the current study, the OC/EC ratio for AQ2 was 1.47 and 1.55 for AQ5, indicating emissions from gasoline vehicles; OC/EC ratios were 1.35, 1.34, 1.24, and 1.19 for AQ1, AQ4, AQ6, and AQ3, respectively, indicating a mix of emissions from diesel and gasoline vehicles [25,26]. The water-soluble ions shown in Figure 3 are comprised of the cations K<sup>+</sup>, Ca<sup>2+</sup>, NH<sub>4</sub><sup>+</sup>, and K-S<sup>+</sup> and anions SO<sub>4</sub><sup>2-</sup> and NO<sub>3</sub><sup>-</sup>. The fraction of K<sup>+</sup> in the form of salt K-S in PM<sub>10</sub> was recorded between 15% to 18% of the total WSI present. The fraction of K<sup>+</sup> in the PM<sub>10</sub> was recorded between 6% to 9% of the total WSI present, and it could be attributed to emissions from refuse or biomass burning, burning of agricultural residue, or burning of fuelwood or cow dung. The percentage of Ca<sup>2+</sup> in ambient PM<sub>10</sub> concentrations was observed between 10% to 14% of the total WSI present; the reason for the presence of Ca<sup>2+</sup> in ambient PM<sub>10</sub> was probably the dust generated from topsoil, roads, and ongoing construction activities surrounding the region. The share of NH<sub>4</sub><sup>+</sup> in ambient PM<sub>10</sub> varied between 10% to 13 % of the total WSI present, which could be attributed to inorganic secondary particulates formed by the chemical reaction of ammonia,

sulphur dioxide, and oxides of nitrogen. In addition, the contributions from the long-range transport of secondary aerosol particles could be attributed to NH<sub>4</sub><sup>+</sup>. The amount of SO<sub>4</sub><sup>2-</sup> varied between 28% to 39% of the total WSI, and it could be attributed to the combustion of diesel and gasoline fuel in vehicles. The share of NO<sub>3</sub><sup>-</sup> in PM<sub>10</sub> was observed between 16% to 21% of the total WSI, with the highest concentration at AQ5, which could be attributed to secondary aerosols formed due to gasoline and diesel combustion in automobiles along with high-temperature fuel combustion in industries or power plants in the upwind regions.

#### 5.4. Elements

The elements investigated in this study were distributed into two groups, namely major elements and trace elements. The major elements, Figure 4, generally include various earth crust elements like Si, Al, Ti, Cl, S, Pb, Na, and Fe. The trace elements shown in Figure 4 include anthropogenic trace markers like Zn, Cr, Br, V, Mn, Ni, and Cu. The major and trace elements could be considered as originating from an anthropogenic or natural source based on the geographical area and travel trajectory of the air mass. In the current study, the major elements contributed to about 28% to 32% of the PM<sub>10</sub> mass, and trace elements contributed to 1% to 2% of the PM<sub>10</sub> mass. The average concentration for the major elements and trace elements is shown in Figure 4. The fraction of Si in ambient PM<sub>10</sub> varied between 38% to 42% of the total major elements, and the fraction of Al was observed between 18% to 21% of the total major elements. The presence of Si and Al in PM<sub>10</sub>



could be because of local dust-generating activities on roads and construction activities. Thus, the presence of Si and Al could be linked to dust generated from fly ash, wind-blown soil, road dust, and construction activities. Other than locally generated dust, the long-range transport of dust was also a probable source contributing to Si and Al [34]. The share of Cl in ambient PM<sub>10</sub> varied between 7% to 10% of the total major elements, which could be attributed to long-range transboundary movement from sea salt-containing particles from the sea [34]. Further, the S and Pb elements were identified as the third most abundant elemental components in ambient PM<sub>10</sub>, with their fractions varying between 6% to 9 % and 6% to 8% of the total major elements, respectively. The urban and regional scale industrial coal combustion, along with the combustion of fuels from vehicles, usually contributes to S and Pb at different locations [09,11]. The other elements observed included the following: Ti, with a proportion of 7% to 9% of the total major elements; Fe, having a fraction between 5 to 7% of total major elements; and Na, with a fraction between 4 to 5 % of total major elements. The sources of Ti and Fe could be traffic exhaust, while the presence of Na could be attributed to fossil fuel combustion in addition to long-range transportation from sea salt [9,11]. If trace elements like Zn, Cr, Br, V, Mn, Ni, and Cu are present in ambient PM<sub>10</sub> in higher concentrations, they can have severe toxic and carcinogenic effects on humans. Of these trace elements, the annual regulatory limits for certain metals like As, Pb, Cd, and Ni have been specified by CPCB [35]. The zinc

proportion varied between 37% to 46 % of the total trace elements, and the source of zinc could be emissions from tire dust, due to the use of zinc in motor oil [9,11]. The fraction of Cr was observed between 25% to 34% of the total trace elements, and the amount of Mn was observed to be between 3% to 5% of the trace element concentration of PM<sub>10</sub>. The combined source of Cr and Mn could be from industrial emissions, especially in steel industries, or emissions from diesel and gasoline combustion [9,11]. The fraction of Br varied in the range of 15% to 18% of the total trace elements, and that of Vanadium varied between 5% to 6% of the trace element concentration. The presence of Br could be related to automobile exhaust, and that of V could be linked to oil combustion when used in automobiles or industries [9,11]. The fraction of Ni was observed in the range of 2% to 3% of the total trace elements, and that of Cu was observed between 1.5% to 2% of the trace element concentration. The presence of Ni was linked to petroleum processing or fossil fuel combustion, and the source of Cu could be inferred as emissions from diesel, petrol, and coal combustion [9,11]. The mean concentration of lead for the six locations was 2257, 2661, 2134, 2347, 2343, and 2086 ng/m<sup>3</sup>, respectively, which exceeded the CPCB limit of 500 ng/m<sup>3</sup>. Pb can be expected from re-suspension of road dust, wearing of vehicle tires, gasoline additives, brake pads, and battery processing units. Similarly, the concentration of Ni at the six locations was found to be 37, 33, 33, 46, 39, and 35 ng/m<sup>3</sup>, respectively, which exceeded the CPCB limit of 20 ng/m<sup>3</sup>.

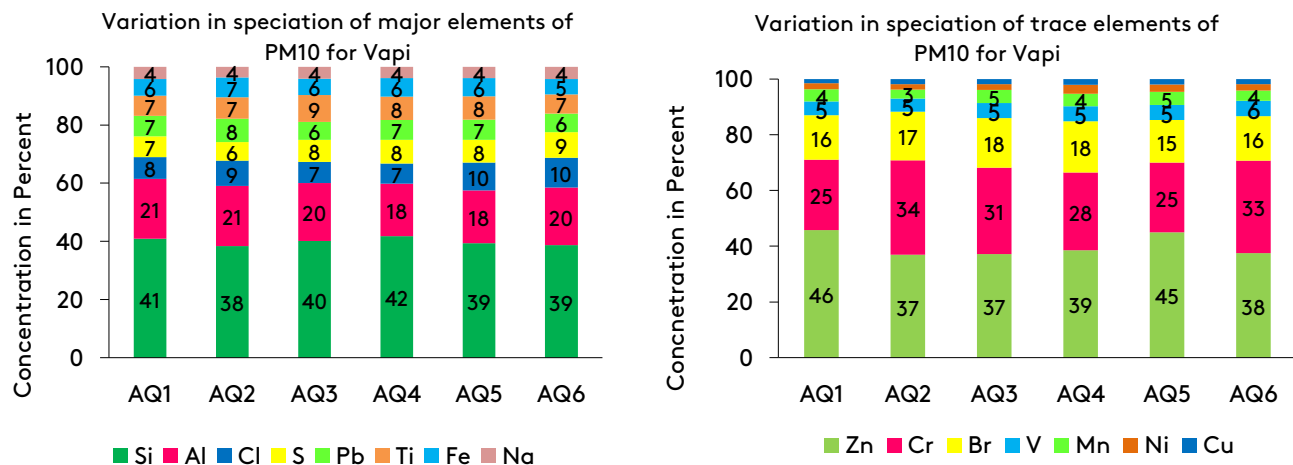


Fig. 4. Variation in speciation of major and trace elements of PM<sub>10</sub> for Vapi.

### 5.5. Source apportionment using CMB

A source apportionment study using CMB model was performed for the Vapi industrial area. The rationale behind this source apportionment study was to recognize possible emissions sources for PM<sub>10</sub> and compute the contributions of sources in the measured ambient concentrations. The estimates of the CMB model are not unique because they are performed based on least-square linear regression; hence, their confirmed accuracy is challenging to establish. The source profiles used in the present CMB model study are selected from the CPCB website developed for Indian metropolitan cities. The emission sources considered are crustal or soil dust, vehicular emissions, secondary aerosols, biomass burning, and fossil fuel combustion, including industries shown in Figure 5. Fossil fuel combustion is the main source of pollution, accounting for 35% of the total emissions for Vapi. A composite source of PM<sub>10</sub> is the burning of any fossil fuel, including coal, natural gas, or oil, light diesel oil (LDO), and heavy diesel oil (HDO). Many marker species have been associated with this source, including Al, SO<sub>4</sub>, Cl, Fe, Cr, and Zn [9]. Crustal or soil dust is the second-largest source of emissions, accounting for 22.90% of the PM<sub>10</sub> mass. Crustal or soil dust is a complex and heterogeneous mixture of dust that can be produced by a variety of activities, including soil dust, resuspended dust, and construction activities [5]. It contains a high concentration of crustal elements like Si, Al, Ca, K, Na, and Mg. EC, OC, Cu, Zn, Mn, Pb, and Ni are the main marker species for vehicular emissions, which is the third-largest source of emissions, contributing 16.18% of the total PM<sub>10</sub> mass [18]. The fourth-largest factor is biomass burning, which has an impact of 19.12%. K<sup>+</sup> is frequently distinguished as a source of burning associated with biomass by the presence of element markers such as SO<sub>4</sub><sup>-2</sup>, NH<sub>4</sub><sup>+</sup>, or OC combined with K<sup>+</sup> [36]. Biomass burning includes a variety of sources, including the burning of domestic fuelwood, agricultural waste, cow dung, solid waste, wildfires, and other biomass waste. The fifth emission source, responsible for 6.79% of emissions, is identified as secondary aerosols, which include ammonium sulphate and ammonium nitrate. Secondary aerosols of atmospheric particles are mostly formed from their

gaseous precursors, such as SO<sub>2</sub>, NO<sub>x</sub>, and NH<sub>3</sub>, and are produced in the atmosphere from both natural and anthropogenic sources [36]. In the current investigation, the CMB model was unable to differentiate industrial emissions as a separate source, as indicated by a higher  $\chi^2$  value. The different performance measures and statistics used for the evaluation of the validity of the CMB model were coefficient of determination (R<sup>2</sup>), chi-square ( $\chi^2$ ), degree of freedom, percent mass, and fit measure [36]. The CMB performance measures for the present study are shown in Table 3.

**Table 3.** Performance measures for CMB.

Sr. No.	Parameter	Value
1	R <sup>2</sup>	0.86
2	$\chi^2$ – Chi-square	15.80
3	Mass percent	95.1%
4	Degree of freedom	14
5	Fit measure	0.72

The value of R<sup>2</sup> ranges between 0.6 to 1, and it is the variance of the measured species concentrations. The higher the value of R<sup>2</sup>, the more the measured concentrations are explained in a better way by source contribution estimates. The weighted sum of squares of the difference between the measured and calculated species concentrations is expressed as chi-square ( $\chi^2$ ). The values of chi-square ( $\chi^2$ ) between 1 and 2 indicate a good and acceptable solution, whereas values greater than 4 suggest an average relationship between species concentrations and selected source profiles for one or more sources [5]. In this case, the  $\chi^2$  value of 15.80 suggested that one source had an average relationship with the species concentration. Hence, by comparison between the CMB and PMF results, the source having an average relationship with the species concentration was the industrial emissions. The percent ratio of the calculated source contribution estimates to the measured mass concentration is termed percent mass, and the values of percent mass ranging between 80 to 120 percent are suggested to represent a good fit of the measured data [5]. The difference between the number of fitting species and the number of fitting sources is expressed as the degree of freedom. As suggested by the CMB manual, the value of the degree of freedom shall be greater than 5 for a reasonable solution.

### 5.6. Source apportionment using PMF

The PMF model was applied for 23 chemical species and 120 PM<sub>10</sub> samples collected during the study period, identifying six prominent sources, namely secondary aerosols, crustal or soil dust, vehicular emissions, industrial emissions, fossil fuel combustion, and biomass burning. The model was run in robust mode to reduce the effect of outliers, and the trial-error method was used to classify the optimum number of sources. The chemical analysis and species distribution of the PM<sub>10</sub> mass identified different sources as secondary aerosols, crustal or soil dust, traffic emissions, industrial emissions, fossil fuel combustion, and biomass burning, as shown in Figure 5.

**Source 1 - Biomass burning:** Emissions from biomass burning constitute about 20% to 30% of coarse particulate matter and are one of the largest sources of organic aerosols [32]. Biomass burning can be considered a fusion of the burning of agricultural residue, fuelwood, cow dung, or forest fires. Potassium is the key marker element used as an inorganic tracer for biomass burning. However, the choice of K<sup>+</sup> as a tracer element for biomass burning may lead to ambiguity with marine aerosols as source signatures. SO<sub>4</sub><sup>-2</sup>, NH<sub>4</sub><sup>+</sup>, or OC in combination with K<sup>+</sup> is often used to differentiate K<sup>+</sup> as a source of biomass-related burning [37]. The PMF analysis revealed a contribution of 14.5% in the present study, with a major contribution from K<sup>+</sup> and SO<sub>4</sub><sup>-2</sup> [32].

**Source 2 - Industrial emissions:** Industrial emissions are usually heterogeneous since the element markers are chiefly associated with the type of industry like petrochemical, pharmaceutical, fertiliser, pesticides, automobiles, etc. The general elemental markers considered for this source include Co, Cu, Cr, Mn, Ni, Zn, etc. [31]. However, the marker elements related to the specific industry include Ni, Cu, and Mn emissions from ferrous or steel industries and emissions like Mn, Cu, and Zn from non-ferrous industries. Various studies indicate the presence of marker elements, namely Ni, Cu, and Zn, from the metallurgical or electroplating industry, and elements like Fe, Mn, SO<sub>4</sub>, Pb, and Zn are associated with smelting operations [9,11]. The elements, namely Ni, S, Cu, and V, result from oil refineries and emissions of Cd, V, and Pb from

battery disposal or refuse oil-related activities. The element markers for the Vapi study area included As, Fe, Cu, Cr, Co, Cd, Mn, S, Ni, and Zn, considering the different industries in the study area included chemical industries, pharmaceuticals, agrochemical industries, pesticide, manufacturing units, paper and pulp industries, dyes, and its intermediate manufacturing units. The contribution from this source was observed to be about ~11.50 % to PM<sub>10</sub> mass, with chief markers being Cr, V, Ni, Cu, Br, and Pb.

**Source 3 - Fossil fuel combustion:** Fossil fuel combustion is a very generic term, which includes the burning of any fossil fuel like coal, petrol, oil, or natural gas. However, the different chemical tracers used to indicate the burning of coal include Cr, Cu, Ni, V, and K [30]. The presence of S, as a coal combustion marker, can also be attributed to the presence of sulphur content in coal, in addition to markers like Al, Si, Zn, and Cl [33]. Similarly, the presence of Se can be linked to oil-fired power plants, while V and Ni can be linked to the combustion of heating or lubricating oils [30,33]. PMF analysis in the current scenario showed that fossil fuel combustion contributed about ~25.75%, with major contributions from EC, OC, Al, Cl, SO<sub>4</sub>, and NO<sub>3</sub>.

**Source 4 - Crustal or soil dust:** It is generally difficult to separate road dust as an individual source of particulate matter since it is found to be a complex and heterogeneous mixture of dust arising from various sources like soil, resuspended soil, construction activities, fuel combustion, vehicular or industrial emissions, etc. The array of crustal elements that are used for source classification as crustal soil dust usually includes Si, Al, Na, Ca, Ti, Mg, and Fe [24,32]. Different researchers have considered soil dust and resuspended soil dust as separate sources [38]. In many studies, dust from construction activities is also considered separately from soil dust. In the current study, soil dust contributed about ~22%, wherein about 49% was from Si and 16% from Al.

**Source 5 - Secondary aerosols:** Very little analysis and study have been done to ascertain the contribution of secondary aerosols to particulates. Past research has revealed that the chief composition of secondary aerosol includes ammonium sulphate and ammonium nitrate,

which are derived from their gaseous precursors, namely ammonium, sulphur dioxide, and oxides of nitrogen [30]. The main markers considered in the category of secondary aerosols usually include ammonium sulphates and nitrates. In this case, PMF analysis showed secondary aerosols contributing about ~9%, with the chief marker elements being  $\text{SO}_4^{2-}$ ,  $\text{NH}_4^+$ ,  $\text{NO}_3^-$ ,  $\text{K}^+$ , and  $\text{Cl}$  [27,32].

**Source 6 - Vehicular emissions:** A series of marker elements, including organic as well as major elements, have been considered for studying the source contribution of vehicular emissions for source apportionment of urban particulates. This source includes composite emissions from different sources like petrol vehicles, diesel vehicles, brake and tire linings, resuspended dust due to vehicle movement, etc. Previous studies have considered the chief markers for this source to be Cu, Zn, Pb, Ni, and Mn [39]. With the introduction of unleaded petrol in the year 2000, the concentration of Pb has been reduced progressively in India; therefore, Pb cannot be considered a distinctive marker of vehicular emissions [14,38]. Many studies have related the presence of EC or OC as elemental markers for diesel emission vehicles. Similarly, the presence of Ca has been linked to the use of different lubricating oils in vehicles [11]. For the Vapi study area, the PMF model analysis represented a contribution of about ~16.95%, where the major contribution came from OC at

61%, 9.7% from Fe, 9.3% from Ca, and about 1.9% from Pb.

Several source apportionment studies have been carried out in different cities of India using CMB and the PMF receptor model [9,11,22]. The summary of the average percentage contribution of major PM sources for PMF and CMB studies undertaken in the Indian context is given in Table 4.

### 5.7. Evaluation of CMB and PMF results

The source signatures obtained from CMB and the PMF model showed a very close correlation, as depicted in Figure 5. The CMB model demonstrated the contribution from the source profiles to be 35% from fossil fuel combustion that included industries, 22.90% from crustal or soil dust, 19.12% from biomass burning, 16.18% from vehicular emissions, and 6.79 percent from secondary particulates. In close link with the CMB results, the outcome of PMF analysis demonstrated the contribution from fossil fuel combustion as 25.75%, the influence from industries being 11.5%, the contribution from crustal or soil dust being 22.13%, the influence of biomass burning being 14.53%, the influence from vehicular emissions being 16.95%, and the contribution of 9.15% from secondary aerosols. Since the CMB model did not differentiate fossil fuel combustion and industries separately, the total contribution from both these sectors was observed as 35%, with the total combination of fossil fuel combustion and industries from the PMF model being 37.23%.

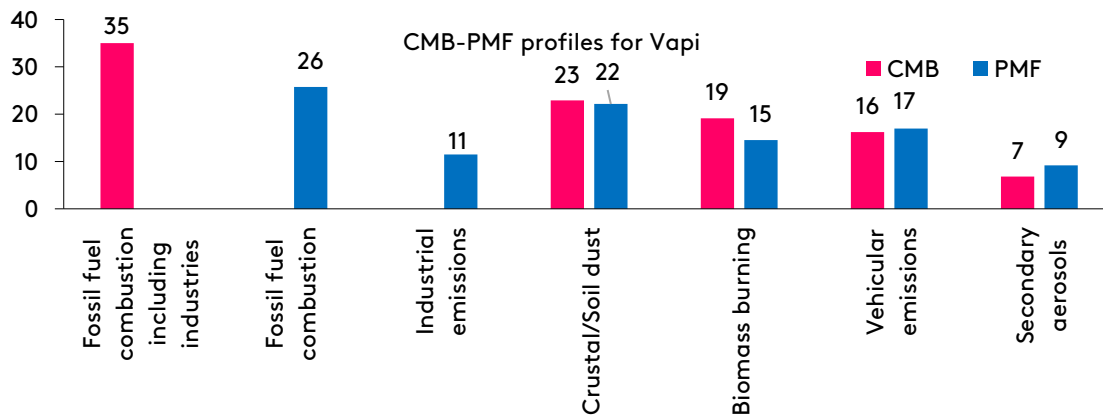


Fig. 5. Source apportionment of the study area using CMB and PMF.

**Table 4 (a).** Summary of the average percentage contribution of PM sources for PMF studies conducted in India.

Sr. No.	Location	PM	Crustal /soil dust	Marine aerosol	Secondary aerosol	Fossil fuel combustion	Industry emissions	Vehicular emissions	Biomass burning	Reference
1	Agra	PM <sub>2.5</sub>	22.45	--	26.2	22.3	--	--	29.1	[6]
2	Agra	PM <sub>2.5</sub>	23.2	--	22.5	26.9	--	--	27.4	[6]
3	Ahmedabad	PM <sub>2.5</sub>	13	--	--	--	11	31	33	[37]
4	Ahmedabad		44	29.8	--	--	13.66	--	--	[28]
5	Chennai	PM <sub>1</sub>	9.43	30.13	20.45	39.99	--	--	--	[22]
6	Chennai	PM <sub>1</sub>	3.4	40.4	22.9	--	12.7	20.1	7	[21]
7	Chennai	PM <sub>2.5</sub>	4.3	21.5	42.1	--	6.8	11.4	14	[21]
8	Dehradun	PM <sub>2.5</sub>	56	--	--	--	50	--	--	[31]
9	Dehradun	PM <sub>2.5</sub>	--	--	--	--	42	62	--	[31]
10	Delhi	PM <sub>2.5</sub>	--	6	23.2	10	--	16	23	[26]
11	Delhi	PM <sub>1</sub>	--	7	21.3	7	--	21	19	[26]
12	Delhi	PM <sub>1</sub>	34	6	8	36	17	--	--	[23]
13	Delhi	PM <sub>1</sub>	16	4	25	14	11	13	17	[25]
14	Varanasi	PM <sub>1</sub>	21	5	20	8	9	18	19	[25]
15	Kolkatta	PM <sub>1</sub>	15	6	25	--	15	18	21	[25]
16	Delhi	PM <sub>2.5</sub>	22.5	4.1	23.2	13.1	6.3	18.5	12.3	[33]
17	Delhi	PM <sub>2.5</sub>	20.5	4.3	21.3	13.7	6.2	19.7	14.3	[8]
18	Delhi	PM <sub>1</sub>	6.2	19.4	38.6	--	4	3.6	6.7	[39]
19	Delhi	PM <sub>2.5</sub>	20.5	4.3	21.3	13.7	6.2	19.7	14.3	[30]
20	Delhi	PM <sub>1</sub>	22.7	4.8	20.5	15.5	7.3	17	12.2	[27]
21	Delhi	PM <sub>1</sub>	20.7	--	21.7	17.4	--	16.8	13.5	[32]
22	Kozhikode	PM <sub>1</sub>	16	25	11	--	--	3	45	[18]
23	Mumbai	PM <sub>1</sub>	26	26	11	16	11	10	--	[16]
24	Mumbai	PM <sub>2.5</sub>	6	12	6	22	13	26	--	[16]
25	Mumbai	PM <sub>1</sub>	27	--	15	17	--	20	--	[24]
26	Mumbai	PM <sub>1</sub>	18	19	--	25	--	23	--	[24]
27	Mumbai	PM <sub>1</sub>	15	16	27	--	--	25	--	[24]
28	Mumbai	PM <sub>1</sub>	19	24	18	--	--	22	--	[24]
29	Patiala	PM <sub>1</sub>	20.7	--	16.2	--	22.9	19	21.2	[25]
30	Vishakhapatna	PM <sub>1</sub>	22.5	9.7	--	15.5	5.1	--	35	[29]
31	Vishakhapatna	PM <sub>1</sub>	22.5	5.5	12.9	26.1	7.8	14	--	[15]

**Table 4 (b).** Summary of the average percentage contribution of PM sources for CMB studies conducted in India.

Sr. No.	Location	PM	Fossil fuel combustion	Crustal / Road dust	Vehicles	Industrial	Refuse/ Field burning	Secondary/ Marine aerosols	Other	Reference
1	Bangalore	PM <sub>10</sub>	4.2	50.6	19	4.5	---	8.7	13	[2]
2	Bangalore	PM <sub>2.5</sub>	5.8	3.5	49.9	3.5	---	12.7	24.7	[2]
3	Delhi	PM <sub>10</sub>	---	64	29	3	---	---	4	[36]
4	Delhi	PM <sub>2.5</sub>	---	35	62	2	---	---	1	[36]
5	Delhi	PM <sub>2.5</sub>	---	35	20	20	16	---	9	[3]
6	Delhi	PM <sub>10</sub>	---	43	17	20	13	---	7	[3]
7	Hyderabad	PM <sub>10</sub>	12	40	22	9	7	---	10	[1]
8	Hyderabad	PM <sub>2.5</sub>	9	26	31	7	6	---	21	[1]
9	Hyderabad	PM <sub>10</sub>	6.1	33.6	43.6	---	6.9	9.7	---	[17]
10	Hyderabad	PM <sub>2.5</sub>	9.7	18.1	35.9	---	16.4	18.8	---	[17]
11	Kanpur	PM <sub>2.5</sub>	13	6	37	---	23	15	---	[4]
12	Kolkata	PM <sub>10</sub>	42	21	---	---	7	---	29	[5]
13	Kozhikode	PM <sub>10</sub>	---	46	18	---	18	17	6	[18]
14	Mumbai	PM <sub>10</sub>	20.6	10	36.3	2.1	---	---	---	[14]
15	Nagpur	PM <sub>2.5</sub>	---	6	57	---	15.1	16	6	[19]

## 6. Conclusions

The current study provides a comprehensive understanding of fine particulate concentration in the Vapi industrial area, along with the elemental speciation of the particulate matter. The results revealed that the mean concentration of PM<sub>10</sub> and PM<sub>2.5</sub> mass exceeded the NAAQS standard values. Further, the mean concentrations of lead and nickel were also found to be exceeding the CPCB limits. The source apportionment study suggested that the CMB model results were fairly comparable with the PMF model results. The CMB model demonstrated the contribution from fossil fuel combustion that included industries to be 35%, whereas PMF revealed a contribution of 25.7% for fossil fuel contribution and 11.5% from industries. The contribution from CMB and PMF for crustal or soil dust was 22.90% and 22.13%, respectively, while those for biomass burning were 19.12% and 14.53%, respectively. The contributions for vehicular emissions were 16.18% and 16.95%, while the contributions for secondary aerosols were 6.79% and 9.15% for the CMB and PMF models, respectively. The present research was useful in analysing the pollution load for a particular area. The outcomes of the study could be used to develop an effective urban air quality mitigation development plan. Considering that the winter season is the worst-case scenario for air pollution dispersion, the current study was taken up only for the winter season. However, future comparative analysis between the summer and winter seasons could be done to produce a more accurate source apportionment study by including monitoring and analysis for the summer season.

## References

- [1] Gummeneni, S., Yusup, Y. B., Chavali, M., Samadi, S. Z. (2011). Source apportionment of particulate matter in the ambient air of Hyderabad city, India. *Atmospheric Research*, 101(3), 752-764.  
<http://doi.org/10.1016/j.atmosres.2011.05.002>
- [2] CPCB, 2010. In: C.P.C.B (Ed.), Air Quality Assessment, Emissions Inventory, and Source Apportionment Studies Bangalore, India. The Energy and Resources Institute, India.
- [3] CPCB, 2010. In: C.P.C.B (Ed.), Air Quality Assessment, Emissions Inventory, and Source Apportionment Studies Delhi, India. *National Environmental Engineering Research Institute*, India.
- [4] Assessment, A. Q. (2010). Emission Inventory and Source Apportionment Studies: Mumbai. *National Environmental Engineering Research Institute, CPCB: New Delhi, India*.
- [5] Gupta, A. K., Karar, K., Srivastava, A. (2007). Chemical mass balance source apportionment of PM<sub>10</sub> and TSP in residential and industrial sites of an urban region of Kolkata, India. *Journal of Hazardous Materials*, 142(1-2), 279-287.  
<http://doi.org/10.1016/j.jhazmat.2006.08.013>
- [6] Agarwal, A., Satsangi, A., Lakhani, A., Kumari, K. M. (2020). Seasonal and spatial variability of secondary inorganic aerosols in PM<sub>2.5</sub> at Agra: Source apportionment through receptor models. *Chemosphere*, 242, 125132.  
<http://doi.org/10.1016/j.chemosphere.2019.125132>
- [7] Nihalani, S. A., Khambete, A. K., Jariwala, N. D. (2020). Receptor modelling for particulate matter: review of Indian scenario. *Asian Journal of Water, Environment and Pollution*, 17(1), 105-112.  
<http://doi.org/10.3233/AJW200012>
- [8] Jain, S., Sharma, S. K., Choudhary, N., Masiwal, R., Saxena, M., Sharma, A., Sharma, C. (2017). Chemical characteristics and source apportionment of PM 2.5 using PCA/APCS, UNMIX, and PMF at an urban site of Delhi, India. *Environmental Science and Pollution Research*, 24, 14637-14656.  
<http://doi.org/10.1007/s11356-017-8925-5>
- [9] Banerjee, T., Murari, V., Kumar, M., & Raju, M. P. (2015). Source apportionment of airborne particulates through receptor modeling: Indian scenario. *Atmospheric Research*, 164, 167-187.  
<https://doi.org/10.1016/j.atmosres.2015.04.017>
- [10] Hopke, P. K., Ito, K., Mar, T., Christensen, W. F., Eatough, D. J., Henry, R. C., Thurston, G. D. (2006). PM source apportionment and health effects: 1. Intercomparison of source apportionment results. *Journal of Exposure Science and Environmental Epidemiology*, 16(3), 275-286.  
<https://doi.org/10.1038/sj.jea.7500458>

- [11] Pant, P., Harrison, R. M. (2012). Critical review of receptor modelling for particulate matter: a case study of India. *Atmospheric Environment*, 49, 1-12.  
<https://doi.org/10.1016/j.atmosenv.2011.11.060>
- [12] GoG (2022), Performance Audit of Air Pollution Control, Comptroller and Auditor General of India, Government of Gujarat.
- [13] GoG (2017) State of Environment, industrial report, Government of Gujarat.
- [14] Chelani, A. B., Gajghate, D. G., Devotta, S. (2008). Source apportionment of PM<sub>10</sub> in Mumbai, India using the CMB model. *Bulletin of Environmental Contamination and Toxicology*, 81(2), 190-195.  
<https://doi.org/10.1007/s00128-008-9453-2>
- [15] Police, S., Sahu, S. K., Pandit, G. G. (2016). Chemical characterization of atmospheric particulate matter and their source apportionment at an emerging industrial coastal city, Visakhapatnam, India. *Atmospheric Pollution Research*, 7(4), 725-733.  
<https://doi.org/10.1016/j.apr.2016.03.007>
- [16] Parthasarathy, K., Sahu, S. K., Pandit, G. G. (2016). Comparison of two receptor model techniques for the size-fractionated particulate matter source apportionment. *Aerosol and Air Quality Research*, 16(6), 1497-1508.  
<https://doi.org/10.4209/aaqr.2015.06.0416>
- [17] Guttikunda, S. K., Kopakka, R. V., Dasari, P., Gertler, A. W. (2013). Receptor model-based source apportionment of particulate pollution in Hyderabad, India. *Environmental Monitoring and Assessment*, 185(7), 5585-5593.  
<https://doi.org/10.1007/s10661-012-2969-2>
- [18] Keerthi, R., Selvaraju, N., Alen Varghese, L., Anu, N. (2018). Source apportionment studies for particulates (PM<sub>10</sub>) in Kozhikode, South Western India using a combined receptor model. *Chemistry and Ecology*, 34(9), 797-817.  
<https://doi.org/10.1080/02757540.2018.1508460>
- [19] Pipalatkhar, P., Khaparde, V. V., Gajghate, D. G., Bawase, M. A. (2014). Source apportionment of PM<sub>2.5</sub> using a CMB model for a centrally located Indian city. *Aerosol and Air Quality Research*, 14, 1089-1099.  
<https://doi.org/10.4209/aaqr.2013.04.0130>
- [20] Belis C. A., Karagulian, F., Larsen, B. R., Hopke, P. K. (2013). Critical review and meta-analysis of ambient particulate matter source apportionment using receptor models in Europe. *Atmospheric Environment*, 69, 94-108.  
<https://doi.org/10.1016/j.atmosenv.2012.11.009>
- [21] Srimuruganandam, B., Nagendra, S. S. (2012). Application of positive matrix factorization in characterization of PM<sub>10</sub> and PM<sub>2.5</sub> emission sources at the urban roadside. *Chemosphere*, 88(1), 120-130.  
<https://doi.org/10.1016/j.chemosphere.2012.02.083>
- [22] Selvaraju, N., Pushpavanam, S., Anu, N. (2013). A holistic approach combining factor analysis, positive matrix factorization, and chemical mass balance applied to receptor modeling. *Environmental Monitoring and Assessment*, 185, 10115-10129  
<https://doi.org/10.1007/s10661-013-3317-x>
- [23] Rai, P., Furger, M., El Haddad, I., Kumar, V., Wang, L., Singh, A., Prévôt, A. S. (2020). Real-time measurement and source apportionment of elements in Delhi's atmosphere. *Science of the Total Environment*, 742, 140332.  
<https://doi.org/10.1016/j.scitotenv.2020.140332>
- [24] Gupta, I., Salunkhe, A., Kumar, R. (2012). Source apportionment of PM 10 by positive matrix factorization in urban area of Mumbai, India. *The Scientific World Journal*, 585791.  
<https://doi.org/10.1100/2012/585791>
- [25] Jain, S., Sharma, S.K., Srivastava, M.K., Chatterjee, A., Singh, R.K., Saxena, M., and Mandal, T.K., (2019). Source apportionment of PM<sub>10</sub> over three tropical urban atmospheres at indo-gangetic plain of India: an approach using different receptor models. *Archives of Environmental Contamination and Toxicology*, 76(1), pp.114-128.  
<https://doi.org/10.1007/s00244-018-0572-4>
- [26] Jain, S., Sharma, S. K., Vijayan, N., Mandal, T. K. (2020). Seasonal characteristics of aerosols (PM<sub>2.5</sub> and PM<sub>10</sub>) and their source apportionment using PMF: A four-year study over Delhi, India. *Environmental Pollution*, 262, 114337.  
<https://doi.org/10.1016/j.envpol.2020.114337>
- [27] Sharma, S. K., Sharma, A., Saxena, M., Choudhary, N., Masiwal, R., Mandal, T. K., &

- Sharma, C. (2016). Chemical characterization and source apportionment of aerosol at an urban area of Central Delhi, India. *Atmospheric Pollution Research*, 7(1), 110-121.  
<http://dx.doi.org/10.1016/j.apr.2015.08.002>
- [28] Raman, R. S., Ramachandran, S., & Rastogi, N. (2010). Source identification of ambient aerosols over an urban region in western India. *Journal of Environmental Monitoring*, 12(6), 1330-1340.  
<https://doi.org/10.1039/b925511g>
- [29] Saggi, G. S., Mittal, S. K. (2020). Source apportionment of PM<sub>10</sub> by positive matrix factorization model at a source region of biomass burning. *Journal of Environmental Management*, 266, 110545.  
<https://doi.org/10.1016/j.jenvman.2020.110545>
- [30] Sharma, S.K., Mandal, T.K., Jain, S., Sharma, A., and Saxena, M., (2016). Source apportionment of PM 2.5 in Delhi, India using PMF model *Bulletin of Environmental Contamination and Toxicology*, 97(2), pp.286-293.  
<https://doi.org/10.1007/s00128-016-1836-1>
- [31] Soni, A., Kumar, U., Prabhu, V., Shridhar, V. (2020). Characterization, source apportionment, and carcinogenic risk assessment of atmospheric particulate matter at Dehradun, situated in the Foothills of the Himalayas. *Journal of Atmospheric and Solar-Terrestrial Physics*, 199, 105205.  
<https://doi.org/10.1016/j.jastp.2020.105205>
- [32] Sharma, S. K., Mandal, T. K., Saxena, M., Sharma, A., Gautam, R. (2014). Source apportionment of PM<sub>10</sub> by using positive matrix factorization at an urban site in Delhi, India. *Urban climate*, 10, 656-670.  
<https://doi.org/10.1016/j.uclim.2013.11.002>
- [33] Sharma, S. K., Mandal, T. K. (2017). Chemical composition of fine mode particulate matter (PM<sub>2.5</sub>) in an urban area of Delhi, India and its source apportionment. *Urban Climate*, 21, 106-122.  
<https://doi.org/10.1016/j.uclim.2017.05.009>
- [34] TERI (2021), Source Apportionment Study and Preparation of Air Quality Action Plan for Surat City, The Energy and Resources Institute (TERI), New Delhi.
- [35] CPCB (2009), National Ambient Air Quality Standards, Central Pollution Control Board.
- [36] Srivastava, A., Jain, V. K. (2007). Seasonal trends in coarse and fine particle sources in Delhi by the chemical mass balance receptor model. *Journal of Hazardous Materials*, 144(1-2), 283-291.  
<https://doi.org/10.1016/j.jhazmat.2006.10.030>
- [37] Sudheer, A. K., Rengarajan, R. (2012). Atmospheric mineral dust and trace metals over urban environment in western India during winter. *Aerosol and Air Quality Research*, 12(5), 923-933.  
<https://doi.org/10.4209/aaqr.2011.12.0237>
- [38] Tiwari, S., Pervez, S., Cinzia, P., Bisht, D. S., Kumar, A., Chate, D. M. (2013). Chemical characterization of atmospheric particulate matter in Delhi, India, Part II: Source apportionment studies using PMF 3.0.
- [39] Singhai, A., Habib, G., Raman, R.S., and Gupta, T., (2017). Chemical characterization of PM 1.0 aerosol in Delhi and source apportionment using positive matrix factorization. *Environmental Science and Pollution Research*, 24(1), pp.445-462.  
<https://doi.org/10.1007/s11356-016-7708-8>